Coupled Simulation of Vapor Flow between Air and a Porous Material

Adam Neale **Dominique Derome** *Member ASHRAE* **Bert Blocken** **Jan Carmeliet**

ABSTRACT

Hygrothermal analysis of buildings is becoming increasingly utilized for evaluating heat and moisture related problems within the building envelope. Convective surface coefficients are particularly important for calculations involving boundary layer heat and mass transfer. As the equations for heat, air and vapor transport within the boundary layer are analogous under particular conditions, the convective moisture coefficients are often calculated through analogy equations, i.e. Lewis and Chilton-Colburn. However, these equations are not always valid. Therefore a different approach is needed to accurately determine heat and mass convection coefficients.

In order to simulate vapor transfer between air and porous materials, this paper presents a model that couples CFD (Computational Fluid Dynamics) with an external vapor transport model developed by the authors. CFD is used to study heat transfer between air and solid materials, because convective transfer coefficients are dependent on the boundary layer velocity and temperature profile. It has been shown that these profiles can be calculated accurately with CFD. Thus, in this paper, CFD models heat and water vapor transport in the air and heat transport within the material. Vapor transport in the material was calculated externally and coupled with the CFD solution at specific time steps. Two cases were simulated using the developed model: 1) a transient case of turbulent air flow over a drying wood sample and 2) a transient case of transitional air flow over gypsum samples.

INTRODUCTION

Convective heat and vapor transfer coefficients, also referred to as surface coefficients, are required to simulate the hygrothermal performance of building envelope systems, for example, in the simulation of the drying of wood or brick cladding wetted by driving rain. Such coefficients can theoretically depend on the following variables: velocity and type of the air flow, surface temperature, reference temperature of the air, surface relative humidity, reference relative humidity of the air and porosity at the surface of the material. Convective heat transfer coefficient correlations are readily available for many geometries and air flow conditions. However, when practitioners refer to codes, standards and handbooks for values of convective heat transfer coefficients, the values provided are often not entirely adequate for their particular case of study. Building physicists face the same problem and must often perform experiments to determine surface coefficients applicable to their particular problem. The information available for the determination of convective vapor transfer coefficients is even more limited even though it has long been a subject of study. Chilton and Colburn (1934) estimated that the boundary layers were similar for heat and moisture flows and proposed an equivalence relation between the heat and mass surface coefficients, which has since been labelled the Chilton-Colburn analogy. Their results, which were later confirmed by Lewis (1970), are used extensively in literature. However, the Chilton-Colburn analogy was developed for particular circumstances, for example in cases without radiation heat transfer, and was then being applied for different types of situations. Many authors have reported values inconsistent with the analogy (e.g. Masmoudi and Prat 1990, Wadsö 1993, Derome 1999, Hukka and Oksanen 1999, Salin 2003,

Adam Neale *is a PhD student and* ***Dominique Derome*** *is an associate professor in the Department of Building, Civil and Environmental Engineering, Concordia University, Montreal, Quebec, Canada.* ***Bert Blocken*** *is an assistant professor of Building Physics and Systems, Technische Universiteit Eindhoven, Eindhoven, The Netherlands.* ***Jan Carmeliet*** *is a professor of Building Physics and Systems, Technische Universiteit Eindhoven, and a professor at the Laboratory of Building Physics, Department of Civil Engineering, Katholieke Universiteit Leuven, Leuven, Belgium.*

etc.). For example, in flows above unsaturated porous materials such as wood, overestimation of the mass transfer coefficient can reach 300% (Derome 1999). However, more accuracy is required as hygrothermal performance simulations have been shown to be sensitive to convective vapor transfer coefficients (e.g. Blocken *et al* 2006).

In terms of experimentally derived surface coefficients, literature provides some data despite the difficulties involved in experimentally determining convective vapor transfer coefficients. Experimental techniques previously used moisture content gradients, gravimetric samples or relative humidity of air to indirectly measure mass flow. More recent techniques such as Particle Image Velocimetry (PIV) and Laser Interferometry (LIF) are expensive but allow accurate boundary layer velocity and mass concentration profiling. Not all testing facilities can afford such equipment, and therefore the accuracy of experimental results is often questionable for a parameter that is so highly dependent on the boundary layer air flow.

As a consequence of the difficulties associated with experimentally measuring surface coefficients and the inadequacy of existing analogies linking convective heat and vapor coefficients, it is desired to find a computer modeling method to accurately determine convective surface coefficients for general conditions seen in buildings.

The objective of this paper is to demonstrate the feasibility and accuracy of using CFD to calculate convective heat and vapor transfer coefficients for conditions required in hygrothermal studies of building envelopes. The determination of surface coefficients requires high-resolution boundary layer solutions, and CFD has been shown in the past to properly resolve air flow for a multitude of problems. In addition, CFD also has the capability to model heat transfer within solids and fluids, though the vapor transport models are generally limited to fluid regions. Due to these reasons, CFD was selected as the computer modeling tool for this research. Specifically, the CFD commercial software *Fluent 6.2.16* was selected to be used for all simulations. Vapor transport in the material was calculated externally and coupled with the CFD solution at specific time steps.

In this paper, the approach taken to simulate the heat and vapor transport associated with the flow of a turbulent air layer over the surface of a porous material is described. First, a review of the definition of surface coefficients is presented. Secondly, the methodology used to determine the convective heat and vapor transfer coefficients within this study is illustrated, followed by a description of the equations used to solve vapor diffusion within the porous material. Some information on CFD is subsequently presented, including the difficulties associated with modeling of vapor transport with CFD. The coupling procedure between CFD and the vapor diffusion model developed by the authors is described, and the results from two case studies are presented. Finally, some concluding remarks are provided.

CONVECTIVE HEAT AND VAPOR TRANSFER COEFFICIENTS

Convective Heat Transfer Coefficient

When considering a fluid flowing over a surface with heat being exchanged, the convective heat transfer can be defined in the following manner:

$$q = -k\frac{\partial T}{\partial y}\bigg|_{y=0} = h_c(T_s - T_f) \qquad (1)$$

where q is the heat flux per unit area (W/m^2), k is the thermal conductivity of the fluid (W/mK), (T/y) is the temperature gradient at the surface (K/m), h_c is the convective heat transfer coefficient (W/m^{2}K), T_s is the surface temperature (K) and T_f is the fluid reference temperature.

Figure 1a illustrates the convective heat transfer process defined in Equation 1. For now, the exact shapes of the velocity and temperature profiles are not considered. Fluid in contact with a surface (i.e. at y = 0 in Figure 1a) has a zero velocity component (no-slip condition) and therefore is assumed to behave via conduction and not convection within that infinitesimally thin layer. Therefore, an energy balance at that location would generally result in Equation 1 governing the heat transfer. However, if radiation is also present, an energy balance would show that Equation 1 is no longer applicable and that the convective heat transfer coefficient must be combined with the radiative heat transfer coefficient. The result is aptly named the combined heat transfer coefficient, which is usually defined by the following relationship:

$$h = h_c + h_R \qquad (2)$$

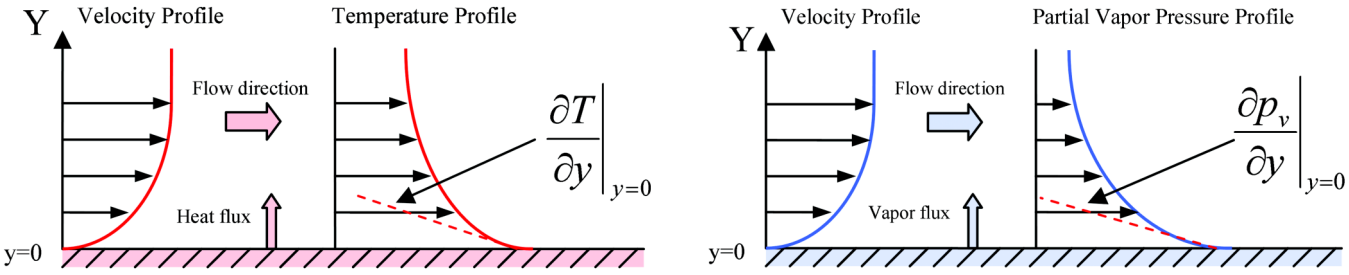

Figure 1 *a) Velocity and temperature profiles for convective heat transfer; b) velocity and partial vapor pressure profiles for convective vapor transfer.*

where h_R is the radiative heat transfer coefficient (W/m^{2}K). The focus of this paper is on convection, and therefore no further discussion of radiation is presented. However, radiation will be included in cases studied in the future.

Convective Vapor Transfer Coefficient

Vapor transfer is considered to be an analogous process to heat transfer for both conduction (i.e. vapor diffusion) and convection. The convective vapor transfer process illustrated in Figure 1b can be defined using an analogous equation to the one presented earlier for heat transfer in Equation 1:

$$g = -\delta \frac{\partial p_v}{\partial y}\bigg|_{y=0} = h_m(p_{vs} - p_{vf}) \tag{3}$$

where g is the mass flux per unit area (kg/m^{2}s), δ is the vapor permeability of the material (s), $(\partial p_v / \partial y)$ is the vapor pressure gradient in the y-direction (Pa/m), p_{vs} and p_{vf} are, respectively, the partial vapor pressure at the surface and the fluid reference vapor pressure (Pa), and h_m is the convective vapor transfer coefficient, which in this case is derived with vapor pressure as the driving potential (s/m).

Experimental determination of convective heat transfer coefficients is generally easier to accomplish than for convective vapor transfer coefficients. This is primarily due to the fact that instruments exist, such as thermocouples, which measure temperature quite accurately at virtually any location in an experiment. Other methods, such as infrared thermography, can determine the temperature distribution for an entire surface in a non-intrusive way. There are no equivalent sensors or equipment for vapor transport quantities. For example, in order to measure partial vapor pressure, both the temperature and the relative humidity must be measured at a given point, and the vapor pressure calculated based upon the data. While partial vapor pressure can typically be measured in air (depending on the experiment), determining the partial vapor pressure for the surface of a material is significantly more complex.

Coupled Heat and Vapor Transfer

Heat and vapor transfer have been described previously as analogous processes, and the implication of the term "analogous" will be defined in this section. Previous work in coupled heat and vapor transfer for experiments and modeling is presented.

To support the description of the combined heat and vapor transfer processes, an example is presented. Let us consider laminar flow over a flat plate with a sharp leading edge, for which an analytical solution can be obtained. The derivation of this solution can be found in most fluid mechanics or heat transfer textbooks. The momentum equation for this case is (*e.g.* Kreith and Bohn 2001):

$$U\frac{\partial U}{\partial x} + V\frac{\partial U}{\partial y} = \nu\left(\frac{\partial^2 U}{\partial y^2}\right) \tag{4}$$

where U is the streamwise velocity (m/s), V is the velocity perpendicular to the plate (m/s), and ν is the kinematic viscosity (m^2/s). Similar equations and solutions exist for temperature and mass concentration. The equations are:

$$U\frac{\partial T}{\partial x} + V\frac{\partial T}{\partial y} = \alpha\left(\frac{\partial^2 T}{\partial y^2}\right) \tag{5}$$

$$U\frac{\partial C}{\partial x} + V\frac{\partial C}{\partial y} = D_{eff}\left(\frac{\partial^2 C}{\partial y^2}\right) \tag{6}$$

where α is the thermal diffusivity (m^2/s), C is the vapor concentration ($kg_{moisture}/m^3_{air}$), and D_{eff} is the effective vapor diffusivity (m^2/s). It should be noted that, while vapor concentration is used in Equation 6, it can be transformed into partial vapor pressure by using the ideal gas law.

The units for kinematic viscosity, thermal diffusivity, and effective vapor diffusivity are all the same. This uniformity highlights the similarities between the three equations presented above. The Prandtl number is defined as the ratio of the kinematic viscosity (ν) to the thermal diffusivity (α). If the Prandtl number were equal to 1, the solutions to the momentum and energy equations would be identical. This leads to the conclusion that the Prandtl number describes the relationship between the velocity and temperature distributions (Kreith and Bohn 2001).

The analogue to the Prandtl number for vapor transport is called the Schmidt number, which is the ratio of the kinematic viscosity to the effective vapor diffusivity:

$$Sc \equiv \frac{\nu}{D_{eff}} \tag{7}$$

The same conclusion can be drawn for the Schmidt number as for the Prandtl number. Since the solution to the momentum and mass concentration equation would be the same if ν were equal to D_{eff}, the Schmidt number must describe the relationship between the velocity and concentration distributions (De Paepe and Steeman 2005).

Another relevant dimensionless term is the Lewis number, which relates the Schmidt and Prandtl numbers, and, as such, also relates the thermal and mass diffusion processes:

$$Le \equiv \frac{Sc}{Pr} \equiv \frac{\alpha}{D_{eff}} \tag{8}$$

The Lewis number describes the last remaining relationship between the three diffusivity terms, namely the ratio between the thermal and vapor diffusion properties.

The three curves shown in Figure 2 represent typical boundary layer profiles for velocity, temperature, and vapor pressure for the case of heat and vapor being transferred via convection from the wall surface to the air layer. The magnitudes of the profiles are not to a particular scale. The variables d, d_h, and d_m represent the boundary layer thickness for, respectively, the velocity, temperature and vapor pressure.

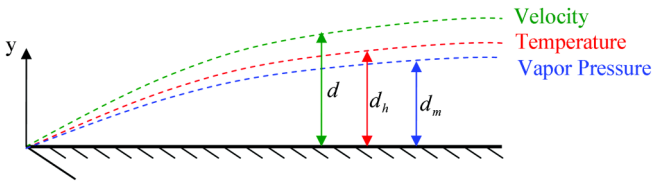

Figure 2 *Superimposed boundary layer profiles.*

Equations are available to determine the boundary layer thicknesses, but are not relevant for the work presented in this paper. For more information, see e.g. Schlichting (1987).

The example shown in Figure 2 illustrates the relative difference between the three profiles. The temperature boundary layer is a function of the velocity boundary layer (via the Prandtl number) and the same holds for the vapor pressure boundary layer (via the Schmidt number). As a result, the temperature profile can be related to the vapor pressure profile. Note that the temperature and vapor pressure curves could also appear above the velocity curve if the Prandtl or Schmidt numbers were greater than unity

What has been briefly described as the relationship between velocity, temperature and vapor pressure, has been transformed into a well known analogy between the convective heat and vapor transfer coefficients (Chilton and Colburn 1934):

$$h'_m = \frac{h_c}{\rho c_p Le^{2/3}} \tag{9}$$

where h_m is the convective vapor transfer coefficient (m/s), h_c is the convective heat transfer coefficient (W/m^{2}K), c_p is the specific heat (J/kgK) and *Le* is the Lewis number. Equation 10 is often referred to as the Chilton-Colburn analogy. The analogy itself has been the subject of many investigations that prove and disprove the accuracy of the results for a variety of conditions. Note that the units of the convective vapor transfer coefficient in Equation 9 are in *m/s*, which are not the same units as for a surface coefficient calculated with vapor pressure as the driving potential. An alternative way of calculating the Chilton-Colburn analogy is to use the following equation:

$$h^*_m = \frac{\delta_a}{k_a} h_c \tag{10}$$

where h^*_m is the convective vapor transfer coefficient (s/m), δ_a is the vapor permeability of air (=1.87x10^{-10} s at 20°C), and k_a is the conductivity of air.

Modeling in Coupled Heat and Vapor Transfer

In addition to experimental work, some modeling of coupled heat and vapor transfer has been performed. The difficulties associated with measurements of vapor transport are most likely the reason why in many cases no model validation was performed. A few examples of numerical modeling of vapor transfer are listed below.

Ben Nasrallah and Perré (1987) developed a coupled heat and mass transfer model for forced convection at the surface of a porous medium. Their model predicted the drying rates for brick at a variety of temperatures, and included a sensitivity study for several parameters. The authors discussed the accuracy of the Chilton-Colburn analogy and stated that it was found to be valid when the vapor pressure of air is negligible with respect to the total pressure. At higher temperatures (60 to 95 °C), they found convective vapor transfer coefficients were up to five times the anticipated values, which is consistent with results from Nabhani *et al* (2003). The model was not compared to experimental data.

Derome *et al* (2003) developed a numerical model to simulate moisture transfer for wood planks in non-vented flat roofs. A sensitivity analysis on the model showed that large variations on the heat transfer coefficients did not result in significant changes in the drying curve for wood. However, when convective moisture transfer coefficients were varied, a larger impact could be seen on the drying process, particularly in the initial stages of drying.

Trujillo *et al* (2003) performed CFD calculations of heat and mass transfer during the evaporation of water from a cylinder for turbulent flow. The simulations did not model vapor transport within the material, only in the air around the cylinder. The results indicated a minimum discrepancy of 19% between the simulated convective heat and vapor transfer coefficients and Chilton-Colburn analogy coefficients. Heat of vaporization was included, and moisture transfer at the surface was modeled using a user-defined function for the moisture concentration. The authors conclude that, at low Reynolds numbers, the Chilton-Colburn analogy is not consistent around the cylinder when the effects of radiation are included.

Hedegaard *et al* (2004) used CFD to simulate moisture transport in both the air and the walls of a room. The walls were modeled as highly viscous fluids due to the inability of the CFD code to model vapor transport in solid materials. Different material properties and viscosities were tested for the viscous wall regions. A number of difficulties were found to be associated with implementing an immobile (yet fluid) region, particularly with turbulence models enabled. Finally, the simulation proved to be too computationally expensive to perform as a transient simulation, and therefore only steady-state simulations were performed.

Erriguible *et al* (2006) simulated the convective drying of a wooden cube in a circular tunnel with the boundary conditions provided by a CFD model. This was for a complex case of air flow over a cube, a case where the determination of the surface coefficients was impossible. CFD was used to provide the boundary conditions to a heat and mass transfer model.

The modeling work found in literature inspired the development of a methodology for the determination of the convective heat and vapor transfer coefficients using CFD coupled with a vapor diffusion model developed by the authors.

CFD AND COUPLED HEAT AND VAPOR TRANSPORT

A number of simulations were performed for forced and natural convection, and the results compared with analytical, semi-empirical or empirical formulae. The convective heat transfer coefficients calculated with CFD have been shown by Neale (2006) to have very good agreement with validation data. Consequently, it was decided to use CFD to perform simulations of coupled heat and vapor transport.

Limitations of CFD with Respect to Vapor Transport

This section will focus on the limitations of general-purpose CFD codes for calculating convective heat and vapor transfer coefficients. The *Fluent 6.3.26* CFD commercial software was used for all of the simulations in this thesis. *Fluent* has the capability to model vapor transport within fluid regions with Species Modeling (Fluent Inc. 2003). However, this capability does not extend to solid regions. This restriction prevents the modeling of diffusive vapor transport within a porous material directly in *Fluent*. Therefore, if CFD is to be used for modeling of combined heat and vapor transport, the models must be modified to include vapor diffusion within the porous materials (Fluent Inc. 2003).

Another limitation of CFD is the limited number of boundary conditions that can be specified for species modeling. The transport variable for species modeling is called mass fraction. The mass fraction for vapor transport in air can be expressed in terms of vapor pressure by using the ideal gas law:

$$X' = \frac{p_v}{\rho_a R_v T} \tag{11}$$

where X' is the mass fraction (kg_{vapor}/kg_{air}), p_v is the vapor pressure (Pa), ρ_a is the density of the air (kg/m^3), R_v is the ideal gas constant for water vapor (= 461.52 J/kgK), and T is the temperature of the air (K).

At the surface of a wall, the mass fraction can be specified as one of two boundary conditions (Fluent Inc. 2003):

1. Zero flux condition: the diffusive vapor flux at the surface of wall is set to zero. This is the default condition for *Fluent*.
2. Specified mass fraction: The user can specify either a constant value that is fixed at the wall surface, which will remain unchanged throughout the simulation, or a user-defined mass fraction boundary profile. The user-defined profile can be based on a user-defined function (for example, an equation that yields mass fraction as a function of position) or a boundary profile that is input from a formatted data file.

The boundary conditions are considered a limitation because a user-defined flux condition different from zero cannot be specified, and a fixed mass fraction boundary condition is not practical for many cases.

Governing Equations

The first governing equation is the continuity equation, which describes how conservation of mass is maintained. In a given two-dimensionally moving fluid, the velocity vector at a given point at a given moment in time can be expressed as the following equation (Lienhard and Lienhard, 2006):

$$\vec{V} = u\vec{i} + v\vec{j} \tag{12}$$

where $\vec{V}$ is the instantaneous velocity vector, u and v are the instantaneous x- and y-components of the velocity (m/s), and $\vec{i}$ and $\vec{j}$ are the unit vectors in the x- and y-directions.

For incompressible flows, the two-dimensional equation that expresses mathematically that a flow is continuous through a given control volume can be expressed as (Lienhard and Lienhard 2006):

$$div(\vec{V}) = \frac{\partial u}{\partial x} + \frac{\partial v}{\partial y} = 0 \tag{13}$$

where *div* is the divergence operator.

For two-dimensional problems, conservation of momentum can be described by two scalar formulae called the Navier-Stokes equations (Lienhard and Lienhard 2006). For CFD modeling, the continuity, momentum and energy equations are lumped together under the "Navier-Stokes" title as a general rule. The Navier-Stokes equations relevant to this paper are presented below in Equations 14a to 14d (see e.g. Ferziger and Peric 1993).

Continuity:
$$div(\vec{V}) = 0 \tag{14a}$$

Momentum:
$$\rho\frac{\partial u}{\partial t} + \rho div(u\vec{V}) = -\frac{\partial p}{\partial x} + div(\mu grad(u)) \tag{14b}$$

$$\rho\frac{\partial v}{\partial t} + \rho div(v\vec{V}) = -\frac{\partial p}{\partial y} + div(\mu grad(v)) \tag{14c}$$

Energy:
$$\rho C_p\left(\frac{\partial T}{\partial t} + \vec{V}\cdot grad(T)\right) = k\nabla^2 T + \dot{q} \tag{14d}$$

where t is the time coordinate (s), p is the instantaneous pressure (Pa), *grad* is the gradient operator, ∇^2 is the Laplacian operator, and $\dot{q}$ is the heat generated (W/m^3). Equations 14a to 14d are valid for any incompressible, two-dimensional, viscous flow of a Newtonian fluid (Blocken 2004).

MODEL COUPLING

Methodology for the Determination of Convective Heat and Mass Transfer Coefficients

In order to simulate vapor transfer between air and porous materials, a model was developed using CFD coupled with an external vapor transport model. CFD was used to model heat and water vapor transport in the air, including both convective and radiative heat transfer, and heat transport within the material. Vapor transport in the material was calculated externally and coupled with the CFD solution at specific time steps.

A transient case of air flow over a drying wood sample was simulated using the developed model. The case that was selected for modeling of heat and vapor transport was for air flow over a porous material. Wood was selected as the material for the porous zones of the model. The general geometry of the cases studied is presented in Figure 3.

In the example shown above, the only process that cannot be solved using *Fluent*, the CFD tool used for this study, is the vapor transport within the porous material. Therefore, a vapor diffusion model was developed to complete the coupled heat and vapor transport model.

Diffusion of Vapor in Porous Materials

The diffusive vapor flux within a solid material was expressed in part earlier in Equation 3. When considering diffusion in a porous material, the storage of moisture must be considered. If one considers vapor transport between two points, the resulting equation can be expressed as:

$$A\frac{\partial w}{\partial t} = \frac{\partial}{\partial x}\left[-\delta A\frac{\partial p_v}{\partial x}\right] \tag{15}$$

where w is the moisture content (kg_{vapor}/m^3), δ is the vapor permeability of the material (s), A is the area perpendicular to the vapor flow, p_v is the partial vapor pressure (Pa), and x is the direction of the vapor flow (m). The gradient $\partial w/\partial t$ represents the vapor storage within the material. Material properties for wood are often expressed in terms of relative humidity, and therefore Equation 15 can be transformed as:

$$A\frac{\partial w}{\partial \phi}\frac{\partial \phi}{\partial t} = \frac{\partial}{\partial x}\left[\delta A p_{vsat}\frac{\partial \phi}{\partial x} + \delta A\phi\frac{\partial p_{vsat}}{\partial T}\frac{\partial T}{\partial x}\right] \tag{16}$$

where ϕ is the relative humidity, p_{vsat} is the saturation vapor pressure (Pa), and the gradient $\partial w/\partial \phi$ represents the slope of the sorption isotherm for the wood. Equation 16 is subsequently applied using a control volume discretization scheme matching the grid used in the CFD simulation.

Coupling Methodology

The equations for vapor diffusion were implemented in *Matlab 7.0*, which is a commercial software used for solving complex mathematical problems. *Matlab* contains integrated solvers for matrix equations, which were particularly useful for determining the relative humidity values for each volume within the domain. Once the routine was programmed into *Matlab*, the procedure to couple the vapor diffusion model with the CFD simulation from *Fluent* was investigated.

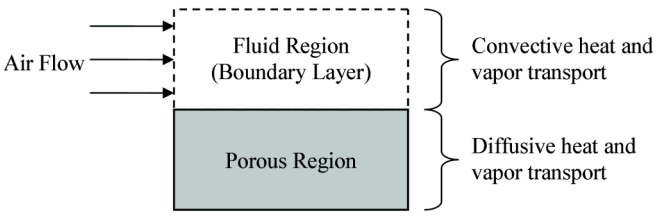

Figure 3 *Domain for convective and diffusive heat and vapor transport.*

Matlab was selected as the controller for the coupled model due to its capability of calling external programs using a command line operator. Even though *Matlab* can run the *Fluent* software, there are still a number of manual steps required to perform a simulation that cannot be accomplished by the controller. For example, a case and data file would have to be opened, the simulation initialized, the number of iterations specified, etc. Such commands cannot be performed directly from *Matlab*. However, they can be automated within *Fluent* through the use of a journal file, which is essentially a list of commands that will be performed sequentially until the end of the file. Given that journal files can automate a simulation and that *Fluent* can be opened from the command line within *Matlab*, all that remained was finding a way to open *Fluent* and directly run a journal file, thus avoiding any manual intervention within *Fluent*.

By using a modified command line, *Fluent* simulations can be performed within *Matlab* using journal files, without ever having to interact with the *Fluent* software during the simulation. However, the simulation parameters must be carefully prepared before this can function properly, and the journal files must contain a number of important commands that prevent the need for user interaction. For example, all dialogue commands that require file-overwrite confirmation must be disabled.

When *Matlab* runs an external program via the command line, it does not recognize whether or not that command has been completed. Programs are executed on a line-by-line basis. The simulations performed in *Fluent* are not instantaneous, and *Matlab* has no built-in method of determining if the simulation was completed or still in progress. The program must either be told to wait for a fixed duration to allow the CFD simulation to reach completion, or it must be told when the program has ended. Due to the variable simulation durations, pausing for a fixed amount of time is prohibitively expensive in terms of computation time. To account for this problem, an external program called Tasklist.exe is utilized. Tasklist is a system tool that can verify whether a particular process is running on a *Windows* operating system. *Matlab* was programmed to call the Tasklist command periodically (every 5 seconds) to verify that the *Fluent* program was still running on the operating system. Once the check was performed and returned a negative result, the program would recognize that the *Fluent* simulation was complete and would proceed with the vapor diffusion calculation.

Another issue that was encountered within *Matlab* was the memory requirements for storing the coefficient matrix from the vapor diffusion equation. The first simulation performed with the model was for a wood region that was subdivided into 38 vertical elements and 100 horizontal elements. The number of elements was equal to the number of

control volumes in the mesh that was created for the CFD simulation. Given that the coefficient matrix has dimensions equal to (m*n)x(m*n), the resulting matrix is 3800x3800 cells, which requires storage of 14.44 million data points. Since the matrix C is a sparse banded matrix, the vast majority of the elements are zero. *Matlab* has the capability to transform a matrix into a sparse matrix, which will only store the non-zero values within the matrix. Through this method, the memory requirements were reduced by an order of about 770, requiring the storage of only 18,724 elements for that particular example.

The flowchart for the solution process for the coupled heat and vapor transfer model is shown above in Figure 4. The data is transferred between each program using data files that are imported and overwritten within *Fluent* and *Matlab*. For example, the mass fraction boundary condition at the surface of the porous material is stored in a file read by *Fluent*, which has a particular format. After the vapor diffusion calculation within *Matlab*, the mass fraction boundary condition for the next time step is written to the same boundary profile file. The program within *Matlab* was designed to write the file in the exact format required by *Fluent*, and, in the case of any errors within the formatting, *Fluent* would return an error and the simulation would end. The six steps shown in Figure 4 are described in further detail below.

1. *Initialization*. The *Fluent* simulation is initialized based on a predetermined journal file. The variables for the general dimensions of the porous material are created and stored in memory.
2. *Air flow and temperature calculation—Fluent*. A CFD simulation is performed for a single time step for air flow and temperature in the air and wood regions. The exact length of the time step is determined in advance by the program or the user. *Matlab* pauses until the CFD simulation is complete and the application is closed via a command in the journal file.
3. *Write data—Fluent*. The relevant mass fraction and temperature profiles are saved to data files. The case and data files are also saved. The *Fluent* application is terminated with the *exit* command.
4. *Vapor calculation—Matlab. Matlab* detects the absence of the *Fluent* application and proceeds to the next part of the program. The output files from *Fluent* that were produced in Step #3 are read into *Matlab*. The mass flux at the surface of the porous region is calculated based upon the difference between the surface boundary condition and the mass fraction at the center of the first cell near the wall. Based upon the mass flux boundary condition, the relative humidity calculation is iterated until a residual of less than 10^{-7} is obtained. Once the relative humidity values are obtained for the current time step, a new mass fraction boundary condition is calculated for the surface of the porous region. The convective vapor transfer coefficients are calculated at this stage for the entire surface of the porous material.
5. *Write data—Matlab*. The boundary condition for mass fraction is written to a profile file in a format that can be input to *Fluent*. The program then verifies that the total simulation duration has not been exceeded. If it has, then the program moves to Step #6, otherwise the program will return to Step #2 and perform additional simulations.
6. *Post Processing*. The post processing stage of the model is still under development. In the present state, the relative

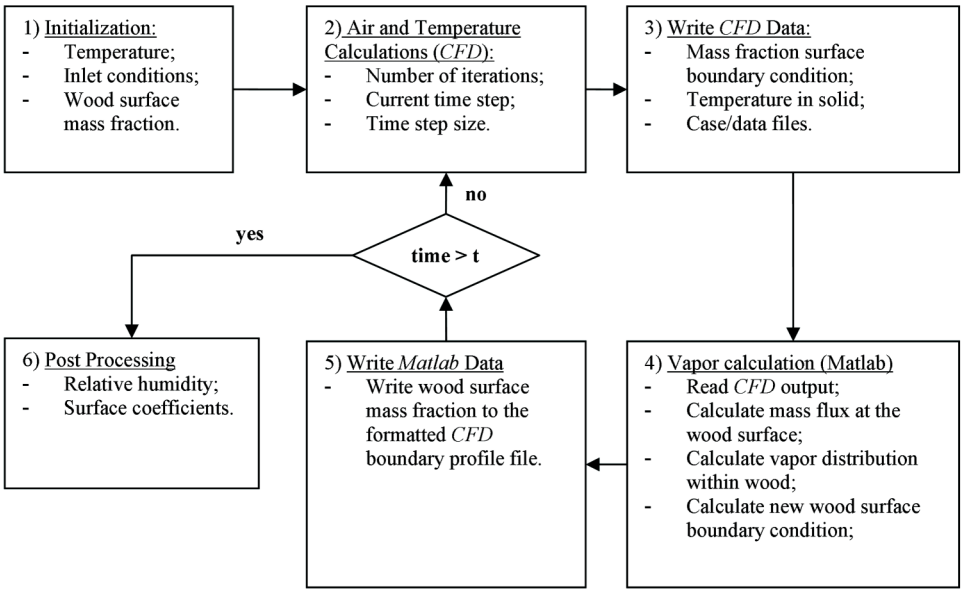

Figure 4 *Coupled model flowchart.*

humidity profiles at specific cross-sections are stored in a matrix for every time step.

APPLICATION OF THE COUPLED MODEL

The coupled model was applied for two separate case studies: 1) a numerical study of air flow over a gypsum bed subjected to moisture adsorption, and 2) a numerical study of turbulent convective drying of wood.

Case 1: Gypsum Panels and Adsorption of Moisture

The first case examines the transient moisture transfer in gypsum panels subjected to convective vapor transport, which corresponds to an experimental study performed by Talukdar and Simonson (2006). The computational domain is shown below in Figure 5.

The velocity profile imposed at the inlet of the domain shown in Figure 5 was a parabolic profile with a bulk speed of 0.82 m/s. The properties of the gypsum were provided by the authors of the experiment, including the relative humidity dependent permeability and the sorption isotherm for the gypsum. The gypsum bed, composed of three layers of gypsum, was assumed to be one homogeneous material with corresponding material properties. The interstitial resistance between the panels is neglected. A portion of the mesh used to spatially discretize the domain is shown in Figure 6.

The time discretization scheme was composed of incremental time steps varying from one second up to a maximum of 600 seconds, which allowed for the comparison of results at 10 minute intervals. The gypsum bed was initialized to approximately 30% relative humidity and the air layer is maintained at a constant 70% relative humidity. The moisture accumulation within the gypsum bed was calculated for each time step. In addition, the viscous model and the bulk speed of the air stream were varied in a sensitivity analysis. The turbulence model used was the Standard *k*- model (Launder and Spalding 1972). The results are presented in the following section.

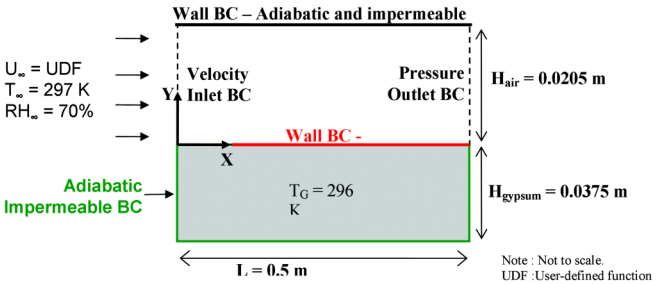

Figure 5 *Computational domain for Case 1.*

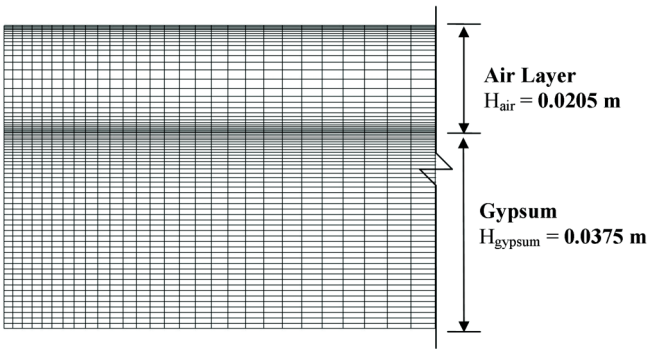

Figure 6 *Mesh used for numerical simulation of Case 1.*

Case 1: Results

The mass of moisture accumulated in the gypsum panels was calculated for four cases: one laminar case at 0.8 m/s bulk flow, and three turbulent cases at 0.8 m/s, 2.0 m/s and 8.0 m/s. Figure 7 demonstrates the sensitivity of the model to the regime of the air flow and to the bulk speed of the air. The case of laminar air flow showed the least accumulation of moisture, with approximately 5 grams after 24 hours. The case with the highest moisture accumulation (7.2 grams) was for turbulent air flow with a higher bulk speed.

Case 1 demonstrated the capability of the coupled model to calculate convective moisture transfer between air and gypsum panels for a number of air flow conditions. Next, a second case of vapor transport between air and a porous material is presented to demonstrate that the coupled model can be used to calculate convective vapor transfer coefficients.

Case 2: Convective Drying of Wood

The second case studied was a numerical simulation of convective drying of wood. The computational domain for Case 2 is presented in Figure 8. The domain is similar to the one used by Neale (2006) for the purpose of validation of

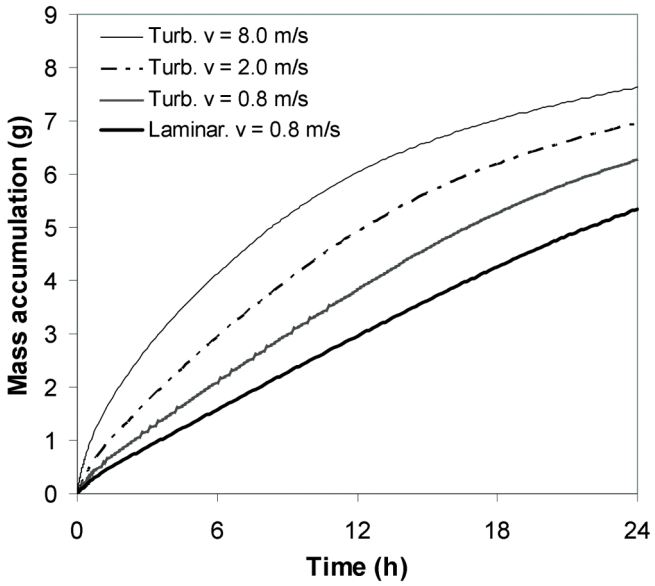

Figure 7 *Mass accumulation for various cases of air flow over gypsum.*

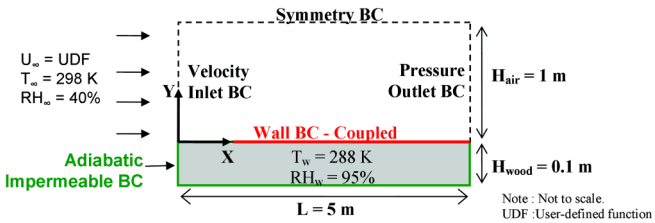

Figure 8 *Domain for convective and diffusive heat and vapor transport.*

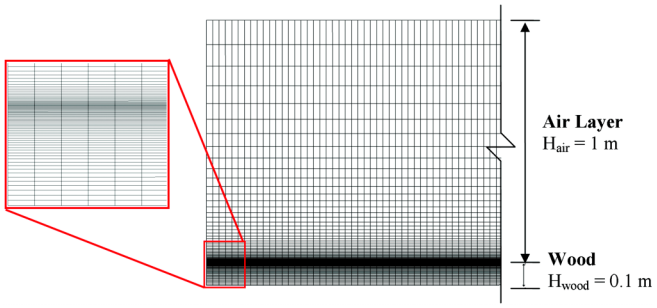

Figure 9 *Mesh used for numerical simulation of Case 2.*

convective heat transfer coefficients for turbulent air flow using CFD. The turbulence model used for the simulations was the *Realizable k-ε* model (Shih *et al* 1995). The near-wall region is solved using the Wolfstein model (Wolfstein 1969). Neale (2006) showed that cases corresponding to the ones studied in this paper give good agreement for convective heat transfer coefficients when compared with empirical correlations.

The mesh used for the simulations is shown in Figure 9. Two time step schemes were used for the simulations: 1) 36 constant time steps of 4800 s and 2) an incremental time step scheme following the relationship described in Equation 17, with an initial time step of 300 s. Two time step schemes were used to test the sensitivity of the model to time discretization. The cases corresponding to the two schemes will be henceforth referred to as Case A and Case B, respectively.

$$t_i = t_1(1+\alpha)^{i-1} \qquad (17)$$

where t_i is the current time step (s), t_1 is the duration of the first time step (= 300 s), and α is a constant (= 0.1271).

Case 2: Results

The accumulated change in mass in the wood is shown in Figure 10 for Case A and Case B. Since the wood is drying, the overall mass of the wood will decrease over time, though the chart below is expressed in absolute values. The graph illustrates the effect of the time discretization on the change in mass of the wood after the full 48 hour drying period. The net difference on the mass accumulation for the two cases is approximately a difference of 8%.

The results are also presented in terms of convective vapor transfer coefficients, h_m. The values of h_m were calculated for every grid cell along the length of the wood surface. The convective heat transfer coefficients, h_c, were also calculated and used to determine a second set of h_m values, denoted as h_m^*, using the Chilton-Colburn analogy described earlier in Equation 9.

Preliminary results indicate that the time discretization scheme selected for the simulation has an important influence on the convective vapor transfer coefficients calculated with the model. The convective heat transfer coefficients do not appear to be significantly affected, though some small differences are noted in the first time steps. Figure 7(a) illustrates the

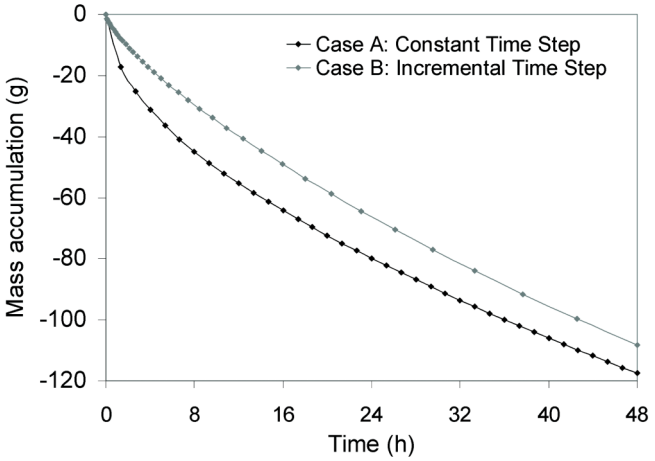

Figure 10 *Moisture accumulation in wood over time.*

convective surface coefficients calculated at the first and last time steps for Case A for the calculated surface coefficients, h_m and h_m^*. Similarly, Figure 11(b) illustrates the same curves, but for the time steps corresponding to the results from Figure 11(a). Due to the incremental nature of the time steps of Case B, the closest time step to 1.33 hours is equal to 1.27 hours.

The results in Figure 11 indicate several trends when comparing convective vapor transfer coefficients (h_m) to values calculated with the Chilton-Colburn analogy (h_m^*). First of all, values of h_m tend to decrease over time and have a short development length (less than 1m). The corresponding curves for h_m^* exhibit the opposite trend, yielding (slightly) increasing values over time with a longer development length. Second, the fixed time step condition yields a larger margin in the values h_m, as seen in Figure 11(a), whereas the h_m values in Figure 11(b) have a smaller margin. Note that the curves for h_m after 48 hours are roughly the same between the two cases, which indicates that the time discretization issue primarily has an impact on the early stages of the simulation. Finally, the decrease in h_m over time seen in both cases indicates that the surface vapor transfer coefficients appear to be dependent upon the moisture content within the material.

Additional simulations demonstrating the effect of time discretization and other influential parameters are still ongoing. A series of simulations using a variety of time and spatial

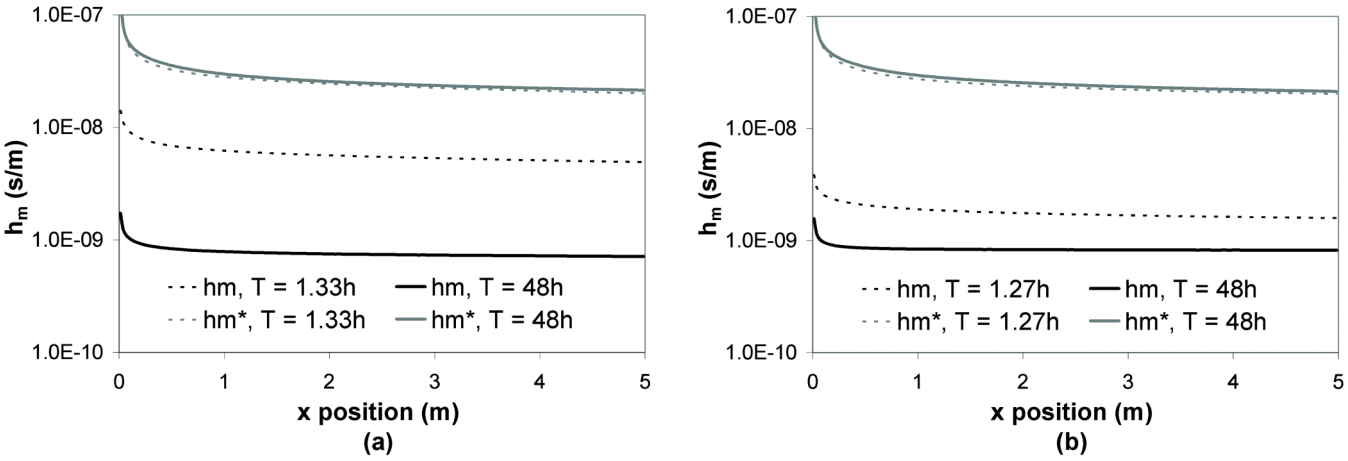

Figure 11 *Convective vapor transfer coefficients for (a) Case A and (b) Case B.*

discretization schemes is currently under study, with the goal of determining the discretization error in the simulation results using Richardson Extrapolation.

CONCLUSIONS

Convective heat and mass transfer coefficients are required to simulate the hygrothermal performance of building envelope systems. A coupling methodology that combines CFD simulations with a vapor diffusion model developed for porous materials was presented for the purpose of calculation convective vapor transfer coefficients. A methodology for externally controlling CFD simulations with an independent program was also presented. The diffusion of moisture was solved with a control volume approach where relative humidity is the driving potential and variations of moisture content follow the desorption-sorption curve. The solution to a number of issues related to external coupling was outlined and the methodology behind the data transfer between CFD and the external model was presented. Two numerical applications of the coupled model were presented in order to illustrate the sensitivity of the model to a number of parameters. A preliminary analysis of the calculated results indicates an overestimation of the convective vapor transfer coefficients derived by the Chilton-Colburn analogy when compared to values calculated directly from the moisture content data in the porous media and air layers.

The coupled model is presented as a work in progress. In the future a number of modifications are intended to be implemented to improve the overall performance. For example, the model currently uses relative humidity as the driving potential for vapor transport, which makes analysis at high moisture content difficult. The model could be modified to use capillary pressure, which would allow for the simulation of a broader spectrum of problems. In addition, equations for the moisture capacity and permeability of wood need to be implemented for a number of temperature ranges and wood species for the full range of moisture contents.

Time discretization appears to have an important impact on the results for the convective surface coefficients calculated with the model. Importance should be placed on the time stepping scheme used to discretize the simulation. Further work in this area is recommended, which could include the implementation of adaptive time stepping to the coupled model.

Finally, no simulation is truly complete without some form of validation. With that purpose in mind, an experimental setup designed by the authors is currently in the construction phase. The experiment is designed specifically for validation of coupled heat and moisture transfer modelling, with careful measurement of the air flow conditions using PIV. Once the experimental setup is complete, validation of the numerical results will provide further insight into the modelling of heat and vapor transport using the proposed coupled model.

REFERENCES

Ben Nasrallah, S., Perré, P. 1988, "Detailed study of a model of heat and mass transfer during convective drying of porous media." Int. J. Heat Mass Transfer 31, 957-967.

Blocken, B. 2004. "Wind-driven rain on buildings," Ph.D. thesis, Leuven: K.U.Leuven.

Blocken, B., Janssen, H., Roels, S., Derome, D., Carmeliet, J. 2006. "A discussion on the formulae for heat and mass surface coefficients in building research." In preparation for Int. J. Heat Mass Transfer.

Chilton, T.H., Colburn, A.P. 1934. "Mass transfer (absorption) coefficients." Industrial and engineering chemistry 26, 1183-1187.

De Paepe, M., Steeman, H-J. 2005. "Heat and mass transfer analogy, limitations and applications to buildings." IEA, Annex 41, Montreal.

Derome, D. 1999. "Moisture occurrence in roof assemblies containing moisture storing insulation and its impact on the durability of the building envelope." Ph.D. Thesis, Montreal: Concordia University.

Derome, D., Fortin, Y., Fazio, P. 2003. “Modeling of moisture behavior of wood planks in nonvented flat roofs.” J. of Architectural Eng., ASCE, 9:26-40.

Erriguible, A., Bernada, P., Couture, F., Roques, M. 2006. “Simulation of convective drying of a porous medium with boundary conditions provided by CFD.” Chemical Engineering Research and Design, 84(A2): 113-123.

Ferziger JH, Peri M. 2002. “Computational Methods for Fluid Dynamics.” Springer, 3rd Edition, 58-60, 2002.

Fluent 6.1 User’s Guide, 2003.

Hedegaard, L., Woloszyn, M., Rusaouën, G. 2004. “Moisture interactions between air and constructions modelled with CFD.” IEA, Annex 41, Glasgow.

Hukka, A., Oksanen, O. 1999. “Convective mass transfer coefficient at wooden surface in jet drying of veneer.” Holzforschung 53, 204-208.

Kreith, F., Bohn, M.S. 2001. “Principles of heat transfer.” 6th Edition, Brooks/Cole.

Launder, B. E., Spalding, D. B. 1972. “Lectures in Mathematical Models of Turbulence.” Academic Press, London, England.

Lewis, J.S. 1971. “Heat transfer predictions from mass transfer measurements around a single cylinder in cross flow.” Int. J. Heat Mass Transfer 14, 325-329.

Lienhard IV, J.H., Lienhard V, J.H. 2006 “A Heat Transfer Textbook”, Phlogiston Press.

Masmoudi, W., Prat, M. 1991. “Heat and mass transfer between a porous medium and a parallel external flow. Application to drying of capillary porous materials.” Int. J. Heat Mass Transfer 34, 1975-1989.

Nabhani, M., Tremblay, C., Fortin, Y. 2003. “Experimental determination of convective heat and mass transfer coefficients during wood drying.” 8th Intl. IUFRO Wood Drying Conference, 225-230.

Neale, A. “A study in computational fluid dynamics for the determination of convective heat and vapour transfer coefficients.” M.A.Sc. Thesis, Concordia University, Montreal, 2006.

Salin, J-G. 2003. “External heat and mass transfer – some remarks.” 8th Int. IUFRO Wood Drying Conference, 343-348.

Schlichting, H. 1987. “Boundary-Layer Theory,” McGraw-Hill, 7th Edition.

Shih, T.-H., Liou, W.W., Shabbir, A., Yang, Z., Zhu, J. 1995. “A new k-e eddy-viscosity model for high Reynolds number turbulent flows – model development and validation.” Computers Fluids, 24(3):227-238.

Talukdar, P., Simonson, C. 2006. “Transient heat and moisture transfer within gypsum.” IEA/ECBCS Annex 41, Kyoto, Japan.

Tremblay, C., Cloutier, A., Fortin, Y. 2000. “Experimental determination of the convective heat and mass transfer coefficients for wood drying.” Wood Science and Technology 34, 253-276.

Trujillo, F.J., Lovatt, S.J., Harris, M.B., Willix, J., Pham, Q.T. 2003. “CFD modeling of the heat and mass transfer process during the evaporation of water from a circular cylinder.” 3rd Int. Conference on CFD in the Minerals and Process Ind., CSIRO, 99-104.

Wadsö, L. 1993. “Surface mass transfer coefficients for wood.” Drying Technology 11, 1227-1249.

Wolfstein, M. 1969. “The velocity and temperature distribution in one dimensional flow with turbulence augmentation and pressure gradient.” Int. J. Heat Mass Transfer 12, 301-318.